



**HAL**  
open science

## An efficient and simple method for investigating dynamic heat transfer in multilayered building components

Emilio Sassine, Yassine Cherif, Emmanuel Antczak, Joseph Dgheim

### ► To cite this version:

Emilio Sassine, Yassine Cherif, Emmanuel Antczak, Joseph Dgheim. An efficient and simple method for investigating dynamic heat transfer in multilayered building components. *International Journal of Masonry Research and Innovation*, 2022, 7 (3), pp.281. 10.1504/ijmri.2022.10046134 . hal-03637177

**HAL Id: hal-03637177**

**<https://hal.science/hal-03637177>**

Submitted on 26 Sep 2022

**HAL** is a multi-disciplinary open access archive for the deposit and dissemination of scientific research documents, whether they are published or not. The documents may come from teaching and research institutions in France or abroad, or from public or private research centers.

L'archive ouverte pluridisciplinaire **HAL**, est destinée au dépôt et à la diffusion de documents scientifiques de niveau recherche, publiés ou non, émanant des établissements d'enseignement et de recherche français ou étrangers, des laboratoires publics ou privés.

# An efficient and simple method for investigating dynamic heat transfer in multilayered building components

Emilio SASSINE<sup>1\*</sup>; Yassine CHERIF<sup>2</sup>; Emmanuel ANTCZAK<sup>2</sup>; Joseph DGHEIM<sup>1</sup>

<sup>1</sup> Lebanese University, Habitat and Energy Unit, Group of Thermal and Renewable Energies - Laboratory of Applied Physics (LPA-GMTER), Faculty of Sciences, Fanar Campus, Lebanon

<sup>2</sup>University of Artois, Laboratory of Civil Engineering and Geo-Environment (LGCgE - EA 4515) Technoparc Futura, F-62400 Béthune, France.

## Abstract

The thermal parameters of building envelopes are crucial information for performing proper building energy simulation, economic optimization, and suitable energy efficiency measures for existing buildings. However, most of the existing building characterization methods require heavy and costly instrumentation equipment as well as relatively long monitoring duration. This paper proposes two new methods for determining the thermal properties of the multilayered building walls: the first method allows the determination of the dynamic thermal properties of each layer separately, while the second method considers an equivalent one-layer homogeneous wall. The two methods are validated using a heating box experimental device with a difference of about 4% for  $\lambda$  and 10% for  $(\rho C_p)$ . Afterwards, a building numerical model is used to compare the two methods showing that the equivalent building components (walls, roofs, and slabs) can be used as accurate and reliable approach for simplifying the difficulty and complexity of thermal identification of multilayered building walls.

**Keywords:** masonry wall, heat modeling, multilayered insulated building, dynamic thermal properties, dynamic heat flow

## NOMENCLATURE

### **Symbols**

$C$	Surface equivalent thermal capacity ( $\text{J.m}^{-2}.\text{K}^{-1}$ )
$C_p$	Specific heat ( $\text{J.kg}^{-1}.\text{K}^{-1}$ )
$e$	Material thickness (m)
$p$	Laplace transform variable (-)
$R$	Thermal resistance ( $\text{m}^2.\text{K W}^{-1}$ )
$T$	Temperature ( $^{\circ}\text{C}$ )
$t$	Time (s)
$E$	Heat transfer matrix of the equivalent wall
$W$	Heat transfer matrix of wall layers
$Z$	Heat transfer matrix of the multilayered wall

### **Greek letters**

$\lambda$	Thermal conductivity ( $\text{W.m}^{-1}\text{K}^{-1}$ )
$\varphi$	Heat flux ( $\text{W m}^{-2}$ )
$\rho$	Density ( $\text{kg.m}^{-3}$ )

### **Indexes**

$amb$	Ambient
$i$	Interior surface
$o$	Exterior surface
$w$	Wall
$ins$	Insulation
$eq$	Equivalent
$exp$	Experimental measured value
$num$	Numerical simulated value

## Highlights

Two numerical methods are proposed and validated for the dynamic thermal characterization of multilayered building walls based on experimental measurements of temperature and heat flux.

The two methods give similar results and are analytically and experimentally validated using an experimental insulated wall.

The sequential identification by layer is recommended when the thermal properties of each layer are needed.

The equivalent wall method is simpler and is recommended when the overall thermal performance of the wall is only needed.

The multilayered and the equivalent building elements numerical methods are compared using a building simulation case study and give similar results.

## 1 Introduction

Improved building envelopes can reduce heating and cooling energy consumption and improve the building energy efficiency. Many research works investigated the heat transfer in multilayered buildings.

Fang et al. [1] proposed a model of coupled heat and moisture (CHM) transfer that allow hygrothermal simulation within porous media in hot and humid climate conditions in China. Ravelo et al. [2] introduced an original modelling of thermal dynamic in the building wall helping to understand the heat transfer mechanism of multilayer walls. The model is based on the Kron's method developed with the Tensorial Analysis of Networks (TAN). Lacarriere et al. [3] studied the unsteady heat transfer in a multi-layer wall including air layers and applied it to vertically perforated bricks.

Even though these works have contributed to a better understanding of heat transfer in multilayered walls, they require knowing the thermal properties of all the building layers beforehand which is not always easy to obtain. In fact, the materials' technical properties are often unknown in existing buildings and in-situ thermal characterization using non-destructive techniques is essential to understand their thermal performance. In addition, in many developing countries, many building materials do not follow strict standardized manufacturing processes and are very often made through traditional craft methods which make their thermal properties unknown and varying in a wide range. Furthermore, although the walls in new buildings have pre-designed thermal performances, it is highly recommended to be able to verify that these performances were met once the construction of these buildings is achieved. The thermal characterization of building walls is thus of great importance in all building cases and is the essential and key step to undertake before performing any building energy simulation, economic optimization, or energy efficiency measures for existing and new buildings.

In general, the thermal characterization techniques can be divided into active techniques where an artificial thermal excitation is used to create specific boundary conditions and passive techniques where there is no artificial intervention to create specific boundary conditions, in this case the outdoor boundary conditions (outside wall surface) have generally a random profile while the indoor boundary conditions (inside wall surface) are almost constant or present very small variations. The passive techniques will be studied in this work due to their ease of implementation and their relatively light and low cost required equipment.

A simple thermal characterization method provided by the ISO 9869 [4] and based on steady-state conditions using only two thermocouples and a heat flux sensor is limited to the determination of the walls' thermal resistance. This method, also known as thermo-fluxmetric method, was used by Bruno et al. [5] to determine the U-value of four different building materials and thin building materials separately. It was also used by Evangelisti et al. [6] and compared to the Air-Surface Temperature Ratio (ASTR) method of building elements in the laboratory steady-state conditions. Desogus et al. [7] compared the thermo-fluxmetric method to a destructive method where a wall sample was drilled and the thermal resistances of the different layers were determined separately. Roque et al. [8] also used the standard ISO 9869 for determining the in situ thermal resistance of a traditional historic building walls in Portugal using the Simple Hot Box - Heat Flow Meter Method

(SHB-HFM) with a baffle integrated inside the Hot Box. Huertas et al. [9] used artificial intelligence techniques to predict the thermal transmittance value walls with monitored data using 163 real monitoring datasets and 140 different typologies of walls from Spain by using the heat flow meter method and the thermometric method. Karthik et al. [10] experimented a test room of 10 cm thick raw rice straw envelope to determine its thermal and moisture diffusivities based on the collected temperature and relative humidity data. Lu et al. [11] adopted an innovative infrared thermography model to determine the thermal resistance of existing walls and compared it with the heat flow meter method. Abdul Nasir et al. [12] studied the impact of building double brick wall construction on the thermal performance of building façade in Malaysia by calculating the wall thermal transmittance (U-values) and the Overall Thermal Transfer Value (OTTV).

The steady state thermal properties of walls (Thermal resistance and thermal transmittance) are generally not sufficient to describe their thermal behavior in dynamic conditions. Dynamic thermal characterization is thus essential for understanding the detailed thermal response of walls in real weather conditions.

Transient heating can be used for determining the dynamic thermal properties of building walls. Chaffar et al. [13] applied a flat resistance heating surface against a 1.8 m x 1.2 m gypsum panel having a thickness of 6.5 cm using infrared thermography for temperature recordings in laboratory conditions and in-situ on a homogeneous reinforced concrete shell. Robinson et al. [14] also used a transient heating method to determine the thermal conductivity and specific heat of a dynamic thermal properties of a 90cm x 90cm x 12cm thick solid concrete wall section. These methods provided relatively accurate results for determining the dynamic properties of the tested walls; however, they present some limitations since they were applied to homogeneous unique layers and they also require specific controlled boundary conditions which may limit their applications in real building scenarios. Yingying et al. [15] used the semi-infinite boundary condition assumption on two traditional multi-layered building wall cases using heating lamps. They measured surface temperatures and heat fluxes, the unit-pulse response and unit-step response only at the front surface for estimating the wall properties. Even though, this method is relatively fast with less than 10 hours, it cannot be generalized to all building walls due to the assumption of semi-infinite wall.

Harmonic boundary conditions [16,17] can also be applied to multilayered walls by assessing the time lag and decrement factor using a hot box and determining the dynamic thermal properties using the EN ISO 13786 [18] standard. However, the method lacks of precision and is limited to harmonic laboratory boundary conditions, making it unsuitable for in-situ measurements. It can also lead to non-precise dynamic properties that are valid to a specific harmonic period.

Among the main works using passive techniques in random dynamic boundary conditions, the study of Gori et al. [19] who used the thermal mass model for determining the dynamic thermal properties of two case studies: an external brick wall in an office building and an aerated clay blocks wall located in a thermal chamber. The method led to satisfactory results, however, the usage of the thermal mass model parameters ( $R_1$ ,  $R_2$ ,  $R_3$ ,  $C_1$ ,  $C_2$ ) in the commonly used building simulation software remains an issue since the common input parameters are the thermophysical properties ( $e$ ,  $\lambda$ ,  $\rho$ , and  $C_p$ ) of each building layer. Petojević et al. [20] used the thermal

impulse response (TIR) functions and the least square estimator based on in-situ measurements to determine the dynamic thermal properties of a multilayered wall. However, some of the results lack of precision with a relative difference of about 30%. Also the same issue of using the thermal characteristics of the wall in building simulation software arises since the TIR functions cannot be used as wall input in most of the existing tools.

The choice of the best methodology for thermal characterization of building walls has been discussed in many research works. Teni et al. [21] presented an overview of the current and most commonly used experimental in-situ approaches for determining the U-value of building walls by dividing them into those that use heat fluxmeters and those that don't. A comparison between internationally standardized and alternative methods is given by assessing their advantages and disadvantages, limitations, and the measurement procedure. Deconinck et al. [22] compared five different characterization methods for determining the thermal resistance of building components using two semi-stationary methods (Average method, Storage effects) and three dynamic data analysis methods (Anderlind, ARX, GREY). They found that the dynamic methods not only converge much faster, but also provide accurate resistance estimates for summer data sets, while the semi-stationary methods did not lead to reliable results for summer measurements. Larsen et al. [23] evaluated the ability of four different in-situ methods (ISO 9869, Modified Average, RC-network and Pentaur methods) to estimate the R-value of four different wall types of a free-running building in a mild climate, under alternating heat flux condition, for different seasons and orientations of the walls. Both simulated and experimental data sets of surface temperatures and heat fluxes were used to analyze the effect of the measuring conditions (surface temperature difference) and the duration of the survey period on the convergence and final R-values.

Nevertheless, there are still many limitations in existing non-destructive thermal characterization methods in real weather conditions. These limitations are mainly related to the determination of the static thermal properties without accounting the dynamic thermal properties [4-12]; as well as the heavy, expensive and cumbersome instrumentation [13-15] used for imposing specific boundary conditions.

This paper studies dynamic heat transfers in multilayered building components by proposing two numerical approaches for determining the equivalent thermal properties of the multilayered building elements using the inverse method technique. This technique is based on the identification between the experimental data and numerical simulations of the heat flux for optimizing the thermal properties of the wall. Two methods are studied: in the first Method (sequential identification by layer), the thermal properties of each layer are computed by starting with the layer in direct contact with the measured heat flux, while the second Method (equivalent wall) considers an equivalent one-layer homogeneous wall that can generate a similar heat flux as the multilayered wall, when subjected to similar boundary conditions.

The proposed method is tested and validated experimentally on an insulated brick wall, and then validated using the analytical thermal quadrupole model. Finally, a building energy simulation using a building case study was used to compare the multilayered wall and the equivalent wall numerical methods.

The originality of the work lies in the numerical approach and the used methods used for the thermal characterization of multilayered building components as well as the model validation through both an analytical study and a dynamic thermal modeling at the building scale. The first method is recommended when the thermal properties of each layer are requested while the second is recommended when the overall thermal performance of the wall is only needed.

## 2 Physical and mathematical model

### 2.1 Physical problem

The general relation of heat transfer for a unidirectional heat flow without an internal heat source is given by the Heat Equation:

$$\frac{\partial^2 T(x, t)}{\partial x^2} = \frac{\rho \cdot C_p}{\lambda} \cdot \frac{\partial T(x, t)}{\partial t} \quad (1)$$

The quadrupole method [18] is based on a 2x2 matrix relating the transform of both temperature and flux on one surface of a considered medium to the same quantities on another surface through networks of impedances:

$$Z = \begin{bmatrix} Z_{11} & Z_{12} \\ Z_{21} & Z_{22} \end{bmatrix} \quad \text{and} \quad \begin{bmatrix} \Theta_{wi} \\ \Phi_{wi} \end{bmatrix} = Z \times \begin{bmatrix} \Theta_{wo} \\ \Phi_{wo} \end{bmatrix} \quad (2)$$

Eq. 2 shows that any two specified temperatures “ $\Theta$ ” or heat fluxes “ $\Phi$ ” boundary conditions (transforms of the appropriate time-dependent boundary conductions) can lead to determine the two others. While the physical problem will dictate which boundary conditions are known, in our case the boundary temperatures  $\Theta_{wi}$  and  $\Theta_{wo}$  are the known parameters, and the internal heat flux  $\Phi_{wi}$  is the unknown parameter.

The heat transfer matrix for a multilayered wall is given by:

$$Z = \begin{bmatrix} Z_{11} & Z_{12} \\ Z_{21} & Z_{22} \end{bmatrix} = W_n W_{n-1} \dots W_3 W_2 W_1 \quad (3)$$

Where  $W_i$  is the matrix of each layer and  $Z$  is the matrix of the equivalent wall.

For the capacitive layers the elements of the matrix  $W_{ij}$  are calculated as follows (ISO13786):

$$W_{11} = Z_{22} = \cosh(\zeta) \times \cos(\zeta) + j \times \sinh(\zeta) \times \sin(\zeta) \quad (4)$$

$$W_{12} = -\frac{\delta}{2\lambda} \times \{[\sinh(\zeta) \times \cos(\zeta) + \cosh(\zeta) \times \sin(\zeta)] + j \times [\cosh(\zeta) \times \sin(\zeta) - \sinh(\zeta) \times \cos(\zeta)]\} \quad (5)$$

$$W_{21} = -\frac{\lambda}{\delta} \times \{[\sinh(\zeta) \times \cos(\zeta) - \cosh(\zeta) \times \sin(\zeta)] + j \times [\sinh(\zeta) \times \cos(\zeta) - \cosh(\zeta) \times \sin(\zeta)]\} \quad (6)$$

With:  $\delta = \sqrt{\frac{\lambda \times P}{\pi \times \rho \times c}}$  and  $\zeta = \frac{e}{\delta}$

Where  $P$  represents the period of temperature variations, in this study a period of one hour (3600s) will be considered in order to be able to model the hourly variations of daily temperature.

For non-capacitive layers (surface exchanges, contact resistances, air gap) the transfer matrix is written as:

$$\begin{bmatrix} 1 & r \\ 0 & 1 \end{bmatrix} \quad (7)$$

Where  $r$  represents the contact resistance.

## 2.2 Thermal identification methods

### 2.2.1 Method 1: Sequential identification by layer (M1)

The thermal properties of each layer are computed by starting with the layer in direct contact with the internal heat flux  $\phi_{wi}$  coming from the heating box as shown in Fig. 1.

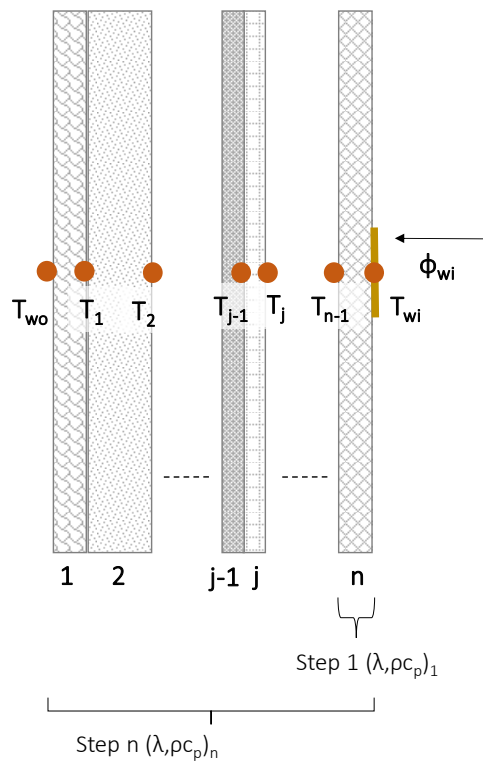


**Figure 1- Sequential identification of multilayered walls**

- First, the thermal properties of layer “n” ( $\lambda$  and  $\rho C_p$ )<sub>n</sub> are determined by comparing the experimental heat flux  $\phi_{wi,exp}$  to the numerical one  $\phi_{wi,num}$  and using as boundary conditions the inside wall surface temperature  $T_{wi}$ ; and the surface temperature at the interface between layer “n” and layer “n-1”,  $T_{n-1}$ .
- Then, the thermal properties of each layer “j”, ( $\lambda$  and  $\rho C_p$ )<sub>j</sub> are determined by comparing the experimental heat flux  $\phi_{wi,exp}$  to the numerical one  $\phi_{wi,num}$ , and using as boundary conditions, the interface surface temperature  $T_j$  between layer “j” and layer “j-1”, and the inside wall surface

temperature  $T_{wi}$ ; and by using the thermal properties of the layer “j+1” → “n” that were determined in the previous optimization phases.

- The process continues until determining the thermal properties of all the layers and by using each time the thermal properties of the previous layers, the experimental heat flux  $\phi_{wi,exp}$ , the inside wall surface temperature  $T_{wi}$ , and the interface surface temperature between the considered layer and the layer adjacent to it.

In the case of a real existing wall, the application of this method supposes the access to the interface between the layers which means the possibility to drill holes in the wall.

### 2.2.2 Method 2: Equivalent wall (M2)

In this method, the overall thermal behavior of the wall matters without the need to determine the thermal properties of the different layers which are usually unknown. This method is very suitable in the case of most of old multilayered (or one-layer) existing walls or the walls that are built with handcrafted construction materials.

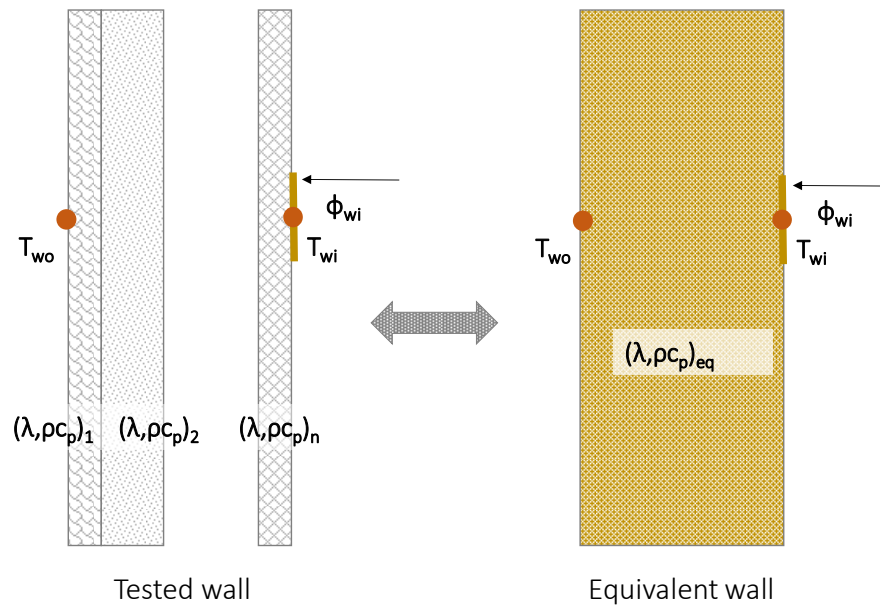


**Figure 2- Comparison between the multilayered wall and the equivalent wall approaches**

These equivalent thermal properties do not relate to any particular material but are representative of the thermal behavior of the wall. The equivalent wall is thus considered as a homogeneous one-layer wall having the same total thickness as the real (multilayered) wall as shown in Fig. 2. This method is much easier, it requires only two thermocouples and one heat fluxmeter, and does not need any access to intermediate wall layers.

### 2.2.3 Relation between methods 1 and 2

The aim of this section is to validate the two methods analytically by relating the thermophysical properties of the equivalent wall ( $e$ ,  $\lambda$  and  $\rho C_p$ )<sub>eq</sub> to the ones of the multilayered wall ( $e$ ,  $\lambda$  and  $\rho C_p$ )<sub>j</sub> supposed to be known, by using complex and automated matrix calculations.

The thickness ( $e$ ) and the thermal conductivity ( $\lambda$ ) of the equivalent wall can be determined by the following relations:

$$e_{eq} = \sum e_j \quad (8)$$

$$\lambda_{eq} = \frac{e_{eq}}{\sum \frac{e_j}{\lambda_j}} \quad (9)$$

The difficulty of the problem relies in determining the thermal capacity ( $\rho C_p$ ) of the equivalent wall. Eq. 2 to Eq. 6 lead to determining the heat transfer matrix “Z” for the multilayered wall:

$$\begin{cases} \theta_i = Z_{11}\theta_e + Z_{12}\phi_e \\ \phi_i = Z_{21}\theta_e + Z_{22}\phi_e \end{cases} \quad (10)$$

$$\phi_i = \frac{Z_{22}}{Z_{12}}\theta_i + \frac{Z_{21}Z_{12} - Z_{22}Z_{11}}{Z_{12}}\theta_e = A\theta_i + B\theta_e \quad (11)$$

$$\text{Where } A = \frac{Z_{22}}{Z_{12}} \text{ and } B = \frac{Z_{21}Z_{12} - Z_{22}Z_{11}}{Z_{12}} \quad (12)$$

The internal heat flux for the equivalent wall can also be expressed in terms of its heat transfer matrix “E”:

$$\Phi_i = \frac{E_{22}}{E_{12}}\theta_i + \frac{E_{21}E_{12} - E_{22}E_{11}}{E_{12}}\theta_e \quad (13)$$

$$\frac{E_{22}}{E_{12}} = f_1(e, \lambda, \rho C_p) \quad (14)$$

$$\frac{E_{21}E_{12} - E_{22}E_{11}}{E_{12}} = f_2(e, \lambda, \rho C_p) \quad (15)$$

In most encountered building scenarios, the indoor temperature is almost constant and set to a predefined temperature while the outdoor ambient temperature varies. Thus, the problem can be simplified to one dynamic boundary condition ( $\theta=0$ ).

In a more generalized definition, two cases can be considered:

- The first case (case 1) where the considered heat flux and the constant temperature are not from the same side; in this case  $\theta_e=0$ .
- The second case (case 2) where the considered heat flux and the constant temperature are from the same side; in this case  $\theta_i=0$ .

The determination of the equivalent wall is thus accomplished according to the following steps:

Step 1: determine the equivalent thickness and the equivalent thermal conductivity from Eq. 8 and Eq. 9.

Step 2: calculate the corresponding terms  $A$  and  $B$  for the multilayered wall (Eq. 10 and Eq. 12).

Step 3: perform the identification between Eq. 11 and Eq. 13 by minimizing the objective function to find the optimal heat capacity. The only parameter to be optimized is  $\rho C_p$ ;  $\lambda$  and  $e$  having already been determined in step 1.

$$F = \sqrt{(f_1(e, \lambda, \rho C_p) - A)^2} \quad \text{if } \theta_e = 0; \text{ (Case A)} \quad \text{or} \quad F = \sqrt{(f_2(e, \lambda, \rho C_p) - B)^2} \quad \text{if } \theta_i = 0; \text{ (Case B)} \quad (16)$$

### 3 Experimental setups

The experimental validation is realized through an insulated masonry brick building wall on which Method 1 and Method 2 are applied.

The multilayered experimental wall is composed of a massive 34 cm thick brick wall having a thermal conductivity  $(\lambda)_w$  and a volumetric heat capacity  $(\rho C_p)_w$ , and a thin 2 cm insulation polystyrene layer having a thermal conductivity  $(\lambda)_{ins}$  and a volumetric heat capacity  $(\rho C_p)_{ins}$ .

The equivalent wall has the equivalent thermal properties  $(\lambda$  and  $\rho C_p)_{eq}$  and has the same total thickness as the multilayered wall. The tested wall and the equivalent wall are represented in Fig. 3.

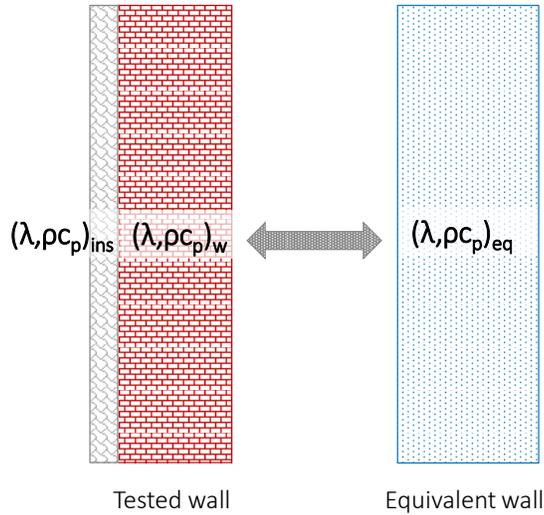


**Figure 3- Tested wall and equivalent wall**

Two experimental setups were adopted; the first one is used for the thermal characterization of sample building materials while the second one uses a heating box and is applied at the wall scale.

### 3.1 Experimental setup for building materials

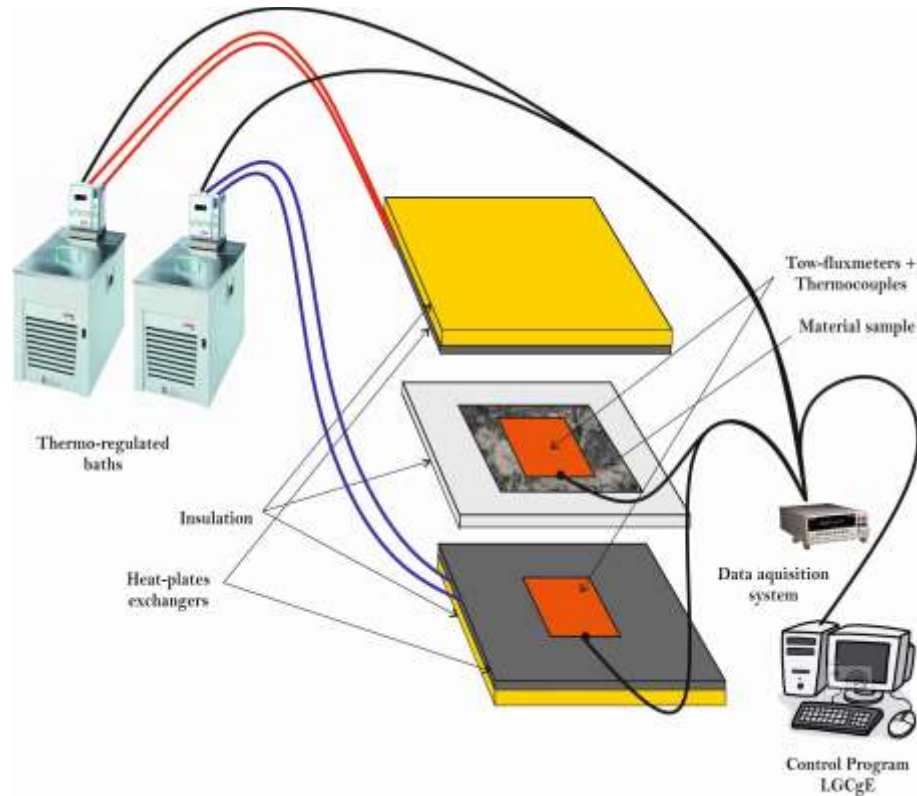


**Figure 4- Thermal characterization setup for building materials**

The experimental device used for thermal characterization of building materials is shown in Fig. 4. It is composed of two thermostatic baths related to two heating plates in order to impose the temperature boundary conditions on the experimented building material. The heat fluxes and the temperatures on both sides of the sample were simultaneously measured using two  $T$ -type thermocouples with a  $\pm 0.1^\circ\text{C}$  precision and two tangential gradient fluxmeters having an active surface of  $0.15 \times 0.15 \text{ m}^2$ . The fluxmeter type is called "tangential gradient fluxmeter", it has a thickness of about  $0.5 \text{ mm}$ , and a sensitivity of about  $100 \mu\text{V}\cdot\text{W}^{-1}\cdot\text{m}^2$  for an active surface of  $15 \times 15 \text{ mm}^2$ . The lateral faces of the sample are covered with an insulation material to apply unidirectional heat transfer conditions.

#### Determination of the thermal conductivity

The method consists in subjecting a sample of thickness " $e$ " to a temperature gradient, so as to impose a flux transfer from the hot side to the cold one. The heat flux and the temperature on both sides of the sample are measured simultaneously. The application of Fourier's law for a unidirectional steady state heat transfer gives:

$$\varphi_{sup} = \varphi_{inf} = \frac{\Delta T}{R} \quad (17)$$

The thermal conductivity can thus be determined by:

$$\lambda = \frac{e}{R} \quad (18)$$

### Determination of the specific heat

Starting from a stable initial steady state, a temperature variation is imposed by changing the set point on one or both sample faces. The average initial temperature of the sample ( $\Sigma T_i/2$ ), as well the fluxes over each side, will change to a new stable state, associated with a new average final temperature ( $\Sigma T_f/2$ ). During this transition, the sample stores or releases heat energy  $Q$  as its temperature increases or decreases. This energy is related to the heat fluxes difference ( $\Delta\varphi$ ) according to the relation:

$$Q = \int_{t_i}^{t_f} \Delta\varphi \cdot dt \quad (19)$$

It can also be related to average temperatures  $\Sigma T_i/2$  at the initial time  $t_i$ , and  $\Sigma T_f$  at the final time  $t_f$ .

$$Q = C \times \frac{\Sigma T_f - \Sigma T_i}{2} \quad (20)$$

The heat capacity of the sample is thus deduced from Eq. (19) and (20):

$$C = \frac{2 \times \int_{t_i}^{t_f} \Delta\varphi \cdot dt}{\Sigma T_f - \Sigma T_i} \quad (21)$$

Knowing the density of the sample and its thickness, the specific heat can be deduced:

$$C_p = \frac{C}{\rho e} \quad (22)$$

### 3.2 Experimental setup for wall testing

The heating box has a thermally controlled atmosphere thanks to a thermostatic bath linked to a radiator with a temperature ranging between 5°C and 60°C. The tested wall is a 34 cm thick masonry brick wall insulated with 2 cm polystyrene panel. The polystyrene panel was well supported against the wall by a wooden frame making it possible to reduce as much as possible the contact resistance between the wall and the insulation (Fig. 5). The choice of a small thickness was made to avoid the limitation of the heat flux which may increase the risk of measurement errors and favor the lateral transfer of the heat flux (2D effect). The lateral wall boundaries were also insulated with 20 cm of Rockwool, which reduces the heat transfer to a unidirectional heat flow. The wall was not submitted to any curing/drying conditions; the relative humidity of the two ambiances (laboratory and heating box) and inside the wall was not monitored and is supposed to be constant. Fig.5 represents a photography of the tested wall (a) and the heating box (b).

Three T-type thermocouples measure the inner and outer wall surface temperatures as well as the temperature at the interface between the insulation and the masonry wall. A heat fluxmeter measures the heat flow across the wall at the inner surface from the heating box side. The sensors are connected to a GL 820 data logger.



**Figure 5- Photography of the tested wall (a) and the heating box (b)**

## **4 Results and discussion**

### **4.1 Experimental results**

#### *4.1.1 Thermal properties of the polystyrene insulation*

The polystyrene sample (Fig. 6) combines two (30 cm x 30 cm) layers; it has a total thickness of 2 cm and weights 111.6 grams. The choice of 4 cm for the thickness instead of 2 cm is due to the fact that this material is very light (31 kg/m<sup>3</sup>), a small thickness therefore risks distorting the specific heat measurements since the sample will store a low amount of energy causing important considerable energy losses (convection inside the measurement enclosure).



**Figure 6- Experimented polystyrene sample**

Four different temperature ranges were used for determining the thermal conductivity of the polystyrene insulation (10°C-20°C, 20°C-30°C, 30°C-40°C, and 40°C-50°C). This allows us to determine the thermal conductivity in function of the average temperature of the sample (Fig. 7). By calculating the conductivity corresponding to the temperatures 15°C, 25°C, 35°C and 45°C, one can obtain an almost straight line as shown in Fig. 8.

The specific heat is computed from Eq. 21 and Eq. 22 and is found equal to  $1392 \text{ J.kg}^{-1}.\text{K}^{-1}$ .

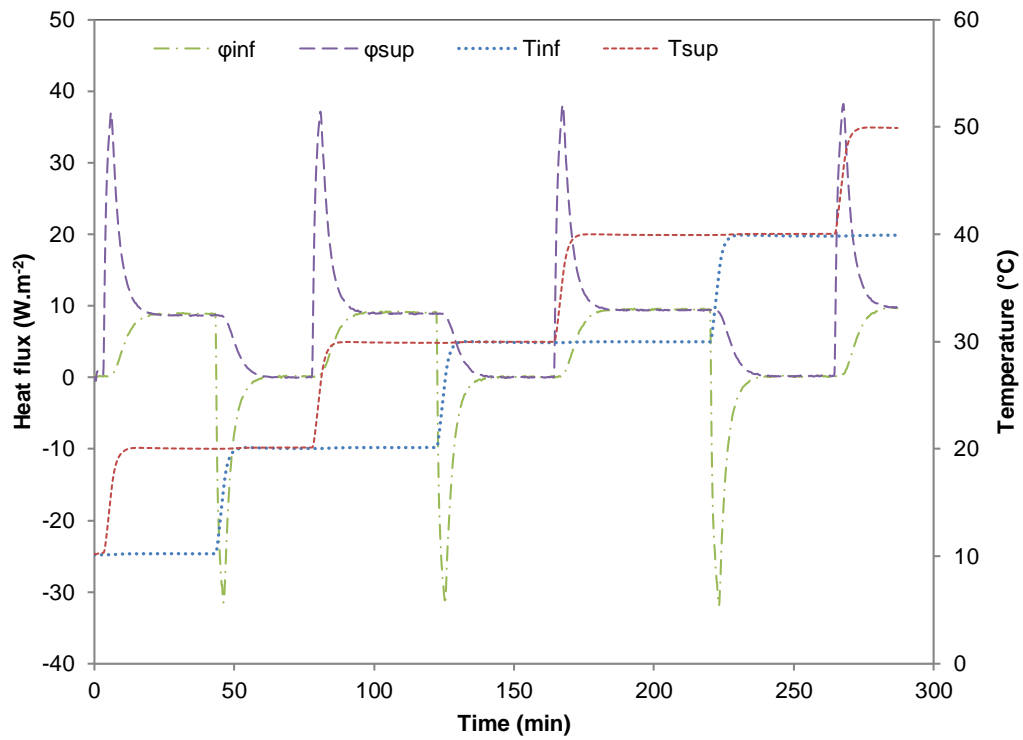


Figure 7- Measured temperatures and heat fluxes at the upper and bottom sample faces

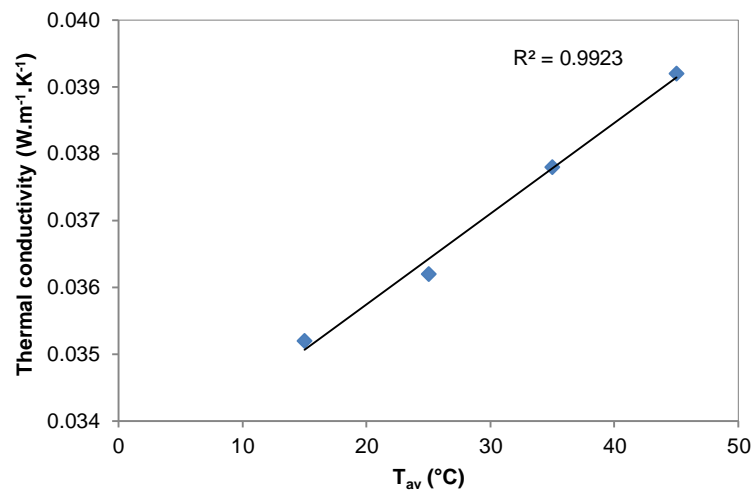


Figure 8- Thermal conductivity of the polystyrene sample for different temperature ranges

#### 4.1.2 Thermal properties of the masonry wall

Masonry walls are heterogeneous components made of blocks and mortar joints; it is therefore necessary to compute the thermal properties of the whole wall (bricks and joints) in order to make it possible to use them in buildings thermal simulation software.

A 6 cm x 11 cm x 22 cm solid brick sample (Fig. 9a) and a 5 cm x 10 cm x 10 cm mortar sample (Fig. 9b) were experimentally tested similarly to the polystyrene sample in order to determine the theoretical thermal properties of the wall. The thermophysical properties of the tested samples are reported in Table 1.



Figure 9- Characterized brick (a) and mortar (b) samples

Table 1- Experimental thermophysical properties of bricks and mortar joints

Material	Density (kg.m <sup>-3</sup> )	Thermal conductivity (W.m <sup>-1</sup> .K <sup>-1</sup> )	Specific heat (J.kg <sup>-1</sup> .K <sup>-1</sup> )
Brick	1505	0.69	620
Mortar	1970	1.41	930

The wall was modelled and simulated using the Finite Element Method in COMSOL Multiphysics® with two different boundary conditions (Fig. 10) for defining its thermal capacity  $(\rho C_p)_w$  and its equivalent thermal conductivity  $\lambda_w$ :

- Stationary study:  $T_1=40$  °C,  $T_2=20$  °C
- Time dependent simulation: initial temperature: 20°C, boundary conditions:  $T_1=T_2=40$  °C.

The thermal conductivity of the wall  $(\lambda)_w$  is calculated from Eq. 17 and Eq. 18 in the stationary simulation study, and the equivalent thermal capacity  $(\rho C_p)_w$  is calculated using Eq. 21, Eq. 22, and the results in Fig. 11 for the time dependent simulation study.

By imposing the stationary boundary conditions, the average heat flux across the wall is 49.58 W.m<sup>-2</sup>, the thermal resistance is thus 0.403 m<sup>2</sup>.K.W<sup>-1</sup>, and the equivalent thermal conductivity is 0.843 W.m<sup>-1</sup>.K<sup>-1</sup>.

The equivalent thermal properties for the brick masonry wall are reported in Table 2.

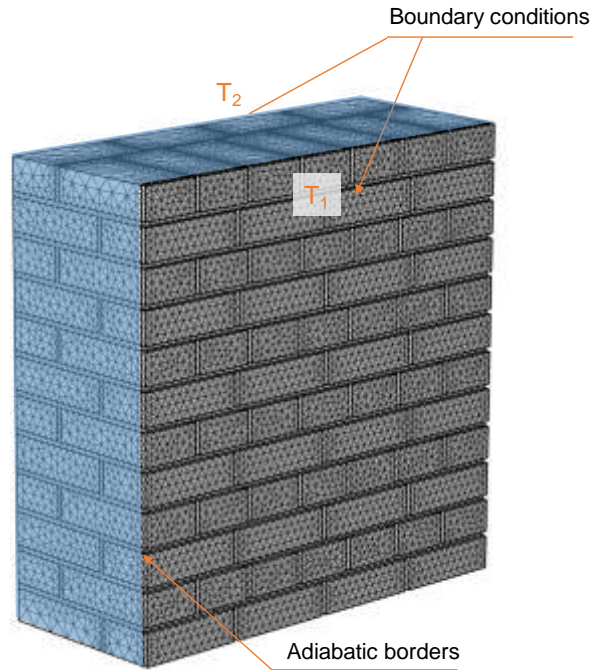


Figure 10- Boundary conditions for the numerical calculation of the equivalent thermal properties of masonry walls

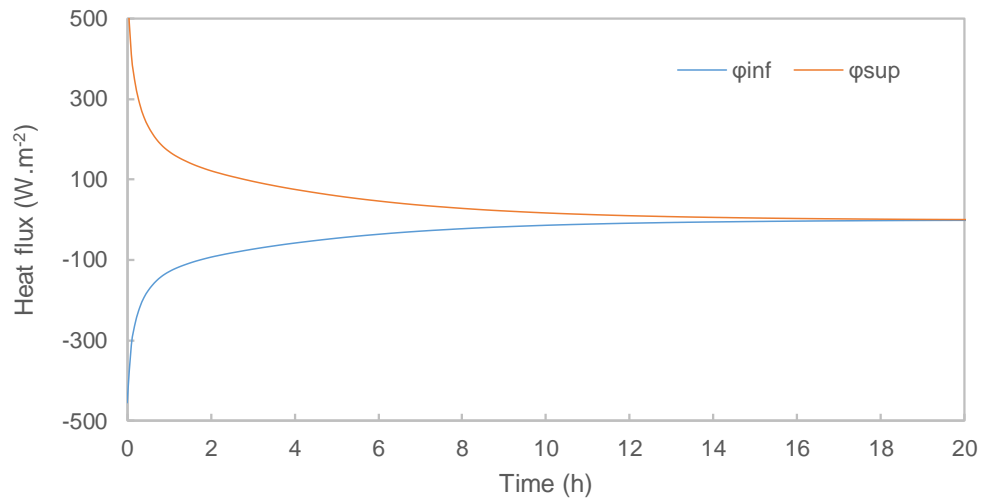


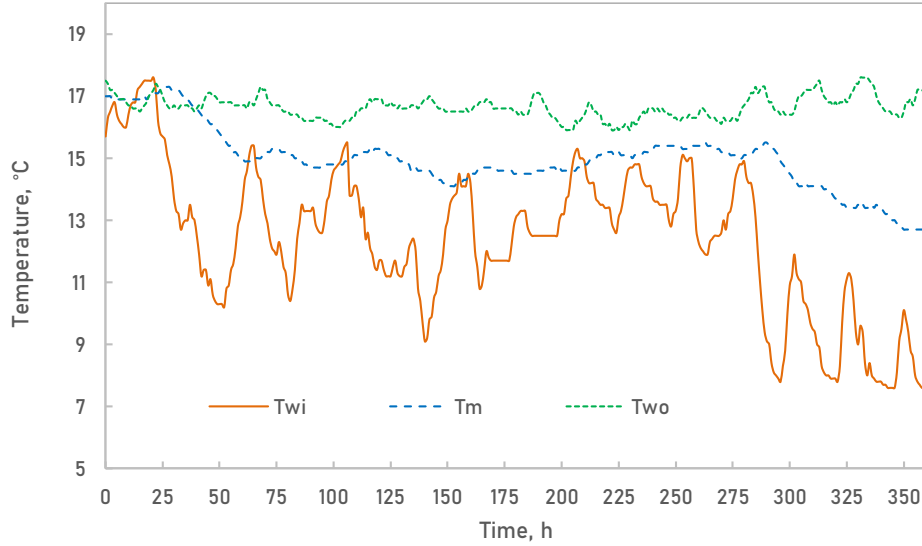
Figure 11- Numerical heat flux evolution for the calculation of the equivalent thermal capacity of the masonry wall

Table 2- Equivalent thermophysical properties of the masonry wall

$(\lambda)_w, W.m^{-1}.K^{-1}$	$(\rho C_p)_w (J.m^{-3}.K^{-1})$
0.843	859657

## 4.2 Validation of the proposed methods

The investigated dataset presents a random temperature profile similar to daily temperature variations with a periodic shape of 24 hours, a time step of 1 hour and a total data logging duration of 360 hours (15 days) as shown in Fig. 12. Very slight variations of  $T_{wo}$  (equivalent to the Laplace transform  $\Theta_e$ ) are observed, which makes it possible to consider only the effect of the inner face temperature  $T_{wi}$  (equivalent to the Laplace transform  $\Theta_i$ ) on the inner flux  $\Phi_i$ .



**Figure 12- Boundary conditions applied to the experimental device for the second random dataset**

The temperature  $T_{wi}$  represents the inner face temperature of the brick wall from the heating box side,  $T_m$  is the temperature at the interface between the brick wall and the insulation material, and  $T_{wo}$  is the outside wall temperature from the laboratory side (polystyrene insulation external face).

In the first method, the temperatures  $T_{wi}$  and  $T_m$  are considered as boundary conditions of the 34 cm brick wall for determining its thermal properties  $(\lambda)_w$  and  $(\rho C_p)_w$  by making the identification between the experimental heat flux  $\varphi_{wi,exp}$  and the numerical one  $\varphi_{wi,num}$ ; then  $T_m$  and  $T_{wo}$  are considered as boundary conditions for the 2 cm insulation material for determining its thermal properties  $(\lambda)_{ins}$  and  $(\rho C_p)_{ins}$  by also making the identification between the experimental heat flux  $\varphi_{wi,exp}$  and the numerical one  $\varphi_{wi,exp}$ .

In the second method, the equivalent wall is considered with a total thickness of 36 cm having temperatures  $T_{wi}$  and  $T_{wo}$  as boundary conditions and the identification between the experimental heat flux  $\varphi_{wi,exp}$  and the numerical one  $\varphi_{wi,num}$  make it possible to determine its equivalent thermal properties  $(\lambda)_{eq}$  and  $(\rho C_p)_{eq}$ .

The optimal thermal properties of the masonry brick wall, the polystyrene insulation, and the equivalent wall are reported in Table 3. The results computed from Method 1 for  $(\lambda)_w$  and  $(\rho C_p)_w$  are close to the equivalent thermophysical properties of the masonry wall (Table 2) with a 14% difference for the thermal conductivity  $(\lambda)_w$  and 11% for the volumetric heat capacity  $(\rho C_p)_w$ . This difference between the results may be due to many factors:

- The sensitivity of the instruments for measurements and especially for the heat fluxmeter.
- The difference between the thermal properties of the bricks; indeed, these blocks are manufactured in a traditional craft way and some difference can be found between the bricks properties.
- The position of the heat fluxmeter of the wall is also a main factor; even though the fluxmeter was placed in the middle of the wall, covering a representative area of brick and mortar joints, the fluxmeter area (15 cm x 15 cm) remains small compared to the wall area and may lead to some measurement errors.
- The 2D heat transfer effect in the wall is also a main challenge leading to some errors even though the wall was well insulated on its lateral surfaces, using a thick massive wall and thermal insulation may cause some undesirable heat losses.
- The influence of moisture content in masonry materials at testing conditions can also be one of the possible factors for the differences found.

Method 1 also succeeded in providing accurate results for the thermal conductivity of the polystyrene with a relative error of about 19% compared to the results of Fig. 8. The main cause of difference between the results of Method 1 and the results of the thermal characterization of the Polystyrene insulation material are due to the relatively thin polystyrene thickness; however, as said before, a thicker insulation may increase the risk of measurement errors and favor the lateral transfer of the heat flux (2D effect). The determination of the volumetric thermal capacity of the polystyrene insulation  $(\rho C_p)_{ins}$  was not possible since this value did not converge. In what follows, the volumetric heat capacity of the polystyrene will be considered  $43000 \text{ J.m}^{-3}.\text{K}^{-1}$  based on the previous thermal characterization results.

**Table 3- Optimal thermal properties  $\lambda$  ( $\text{W.m}^{-1}.\text{K}^{-1}$ ) and  $\rho C_p$  ( $\text{J.m}^{-3}.\text{K}^{-1}$ )**

Method 1	$(e)_w$ , m	0.34
	$(\lambda)_w$ , $\text{W.m}^{-1}.\text{K}^{-1}$	0.981
	$(\rho C_p)_w$ , $\text{J.m}^{-3}.\text{K}^{-1}$	762000
	$(e)_{ins}$ , m	0.02
	$(\lambda)_{ins}$ , $\text{W.m}^{-1}.\text{K}^{-1}$	0.043
	$(\rho C_p)_{ins}$ , $\text{J.m}^{-3}.\text{K}^{-1}$	-
Method 2	$(e)_{eq}$ , m	0.36
	$(\lambda)_{eq}$ , $\text{W.m}^{-1}.\text{K}^{-1}$	0.425
	$(\rho C_p)_{eq}$ , $\text{J.m}^{-3}.\text{K}^{-1}$	1882000

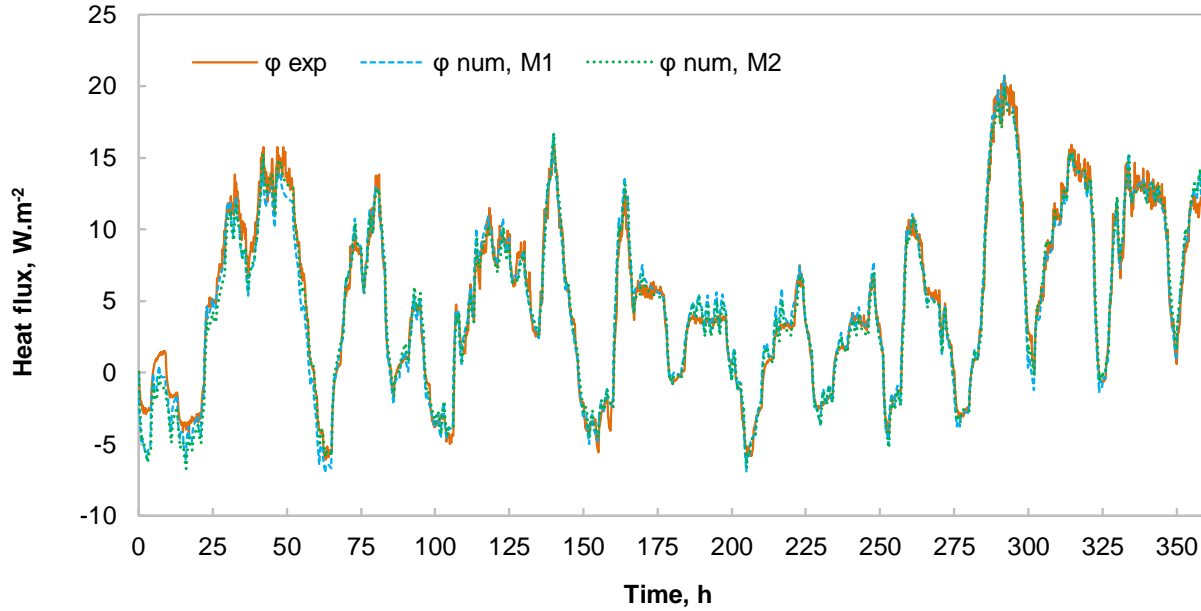


**Figure 13- Comparison between experimental and numerical heat fluxes for the optimal solutions of the two methods**

Fig. 13 clearly shows that the numerical heat fluxes computed using Method 1 with the optimized thermal properties of the brick masonry wall and the polystyrene insulation, and Method 2 using the optimized thermal properties of the equivalent wall, are very similar to each other and also compared to the experimental measured heat flux.

The Nash-Sutcliffe efficiency coefficient (NSE) defines how well the measured and simulated heat fluxes are identical and how well the plot of measured versus simulated model data fits the 1:1 line. A value of  $NSE=1$ , corresponds to a perfect match of the model to the measurements [24].

$$NSE = 1 - \frac{\sum_{i=1}^n (OBS_i - SIM_i)^2}{\sum_{i=1}^n (OBS_i - \overline{OBS})^2} \quad (23)$$

Where “ $OBS_i$ ” is the observed (or measured) value and “ $SIM_i$ ” is the simulated value.

Fig. 14 shows that the  $NSE$  coefficient is close to 1 for Method 1 and Method 2 proving that both methods provide comparably accurate results.

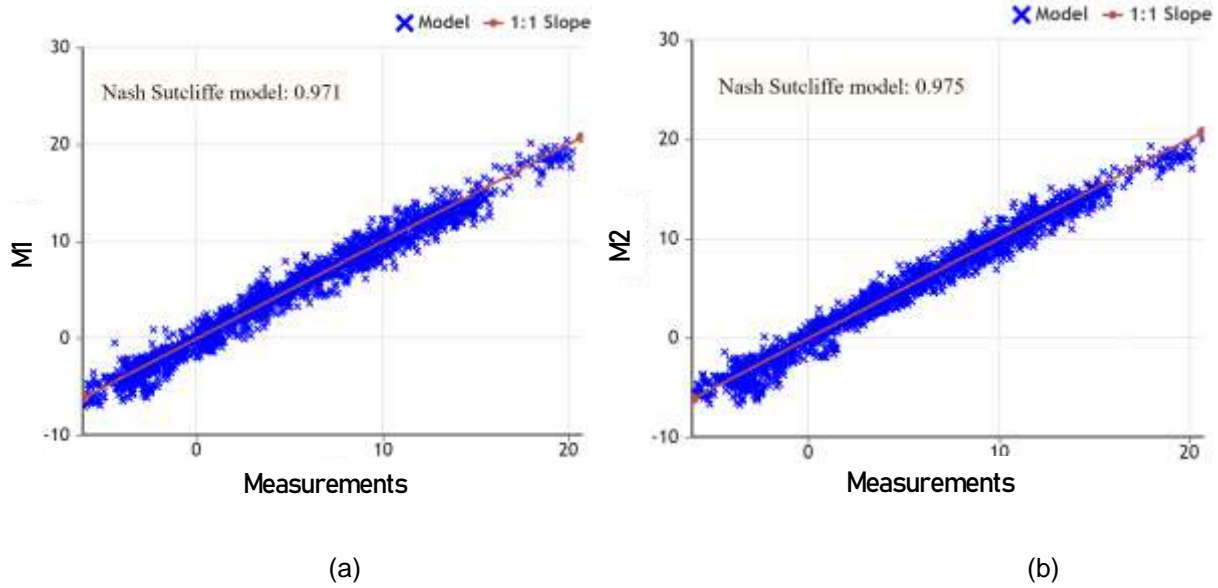


Figure 14- Nash Sutcliffe Efficiency coefficient (NSE) for Method 1 (a) and Method 2 (b)

#### 4.3 Analytical comparison of the results

The aim of the analytical validation is to compare Method 1 and Method 2 from an analytical point of view and demonstrate that the results of the two methods are equivalent. To do so, the equivalent transfer matrix  $Z$  is computed by using the transfer matrixes of the masonry wall and the insulation layer (Eq. 4-7). Afterwards, Eq. 8-16 are used for determining the equivalent thermal properties of the wall and considering Case 1 ( $\Theta_e=0$ ) since the heat flux  $\varphi_i$  (from the heat box side) and the constant temperature  $T_e$  (from the laboratory side) are not from the same side. The results are reported in Table 4. The equivalent thermal properties deduced analytically from the respective thermal properties of the wall and the insulation material that were determined in Method 1 are summarized in Table 4.

The results of the thermal properties of the equivalent wall computed from Method 2 are similar to the equivalent thermal properties from the proposed analytical method using the thermal properties of the masonry wall and insulation layer of method 1. In method 2, the equivalent thermal conductivity and volumetric heat capacity are  $0.425 \text{ W}\cdot\text{m}^{-1}\cdot\text{K}^{-1}$  and  $1882000 \text{ J}\cdot\text{m}^{-3}\cdot\text{K}^{-1}$  respectively (Table 3), while the equivalent thermal properties computed from the results of Method 1 are  $0.444 \text{ W}\cdot\text{m}^{-1}\cdot\text{K}^{-1}$  and  $1685457 \text{ J}\cdot\text{m}^{-3}\cdot\text{K}^{-1}$  (Table 4) with a difference of about 4% for  $\lambda_{eq}$  and 10% for  $(\rho C_p)_{eq}$ .

It is also important to mention that the coefficient of  $\Theta_e$  is very low compared to the coefficient of  $\Theta_i$  which is due to the fact that the wall is very thick and insulated from the outside making the effects of the temperature variations from the outside of the heating box negligible compared to the temperature variations from the side of the heating box. Also, the effect of varying the volumetric heat capacity of the insulation material  $(\rho C_p)_{ins}$  on the equivalent volumetric heat capacity of the insulated wall  $(\rho C_p)_{eq}$  was found to be very negligible which

confirms that the latter parameter is not sensitive to the value of  $(\rho C_p)_{ins}$ ; this explains why the volumetric heat capacity of the insulation material in Method 1 did not converge.

**Table 4- Analytical determination of the equivalent thermal properties of the wall**

$e_w$ (m)	0.34
$\lambda_w$ (W.m <sup>-1</sup> .K <sup>-1</sup> )	0.981
$(\rho C_p)_w$ (J.m <sup>-3</sup> .K <sup>-1</sup> )	762000
$e_{ins}$ (m)	0.02
$\lambda_{ins}$ (W.m <sup>-1</sup> .K <sup>-1</sup> )	0.043
$(\rho C_p)_{ins}$ (J.m <sup>-3</sup> .K <sup>-1</sup> )	42000
$e_{eq}$ (m)	0.36
$\lambda_{eq}$ (W.m <sup>-1</sup> .K <sup>-1</sup> )	0.444
$(\rho C_p)_{eq}$ (J.m <sup>-3</sup> .K <sup>-1</sup> )	1685457

## 5 Determination of equivalent building components at building scale

The interest of the building simulation analysis is to validate that the assumptions of considering the inner wall temperature constant, and also to prove that the equivalent wall can replace the multilayered wall in real building context with real weather conditions.

### 5.1 Building case study

The studied building case is a Townhouse, a typical building typology widespread in the “Flanders region” in Western Europe including the North of France, Belgium, Netherlands, and a part of Germany.

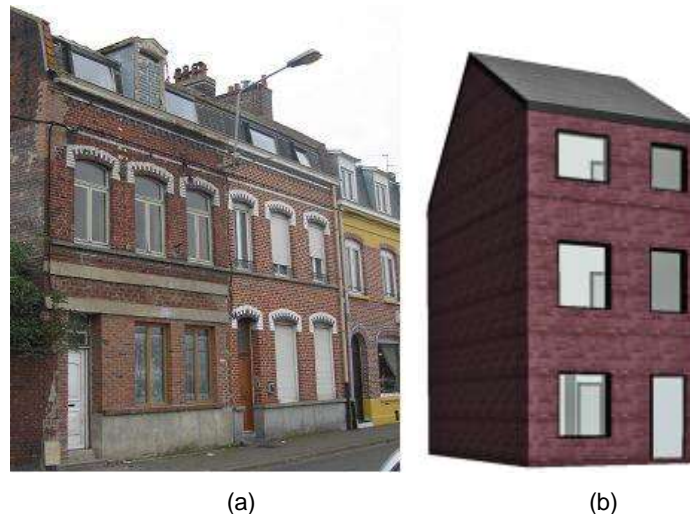


**Figure 15- Photography (a) and model (b) of the simulated town house**

Townhouses often have the same layout: an entrance door and a side corridor, then, in a row, the dining room, the kitchen and the veranda or garden. Upstairs, one or two bedrooms and a bathroom and then an attic floor containing one or two bedrooms (Fig. 15). These old buildings are often adapted to current comfort standards

(sanitary, heating, insulation, etc.). They have a living area between 90 and 130 m<sup>2</sup> and often an added extension. The townhouse traces the axes of the city, streets, avenues, and boulevards; it is located between two adjoining houses on a narrow (4 to 7 meters) and elongated (10 to 20 meters) plot.

## 5.2 Simulation assumptions

TRNSYS Software was used for dynamic building energy simulation. Surface temperatures and heat fluxes for the different building envelope components were chosen as outputs in addition to the total sensible heat and the indoor air temperature. A simplified building model was considered with one unique thermal zone. The chosen base temperatures are 20°C for heating and 24°C for cooling. The case study building was considered to be reasonably tight with an air change rate of about one change per hour.

The Type 56 component was used to model the thermal behavior of the building using a pre-processing program, the TRNBUILD program for creating the so-called building file. The user describes each thermal zone using with some basic project data, and then selects the desired outputs.

The weather file of Uccle, one of the municipalities located in the Brussels-Capital Region of Belgium, was considered. The average daily temperature per month as well as the average daily horizontal solar radiation per month, are shown in Fig. 16. The average daily temperature per month is less than 20°C for all months which confirms that no cooling is necessary in this region.

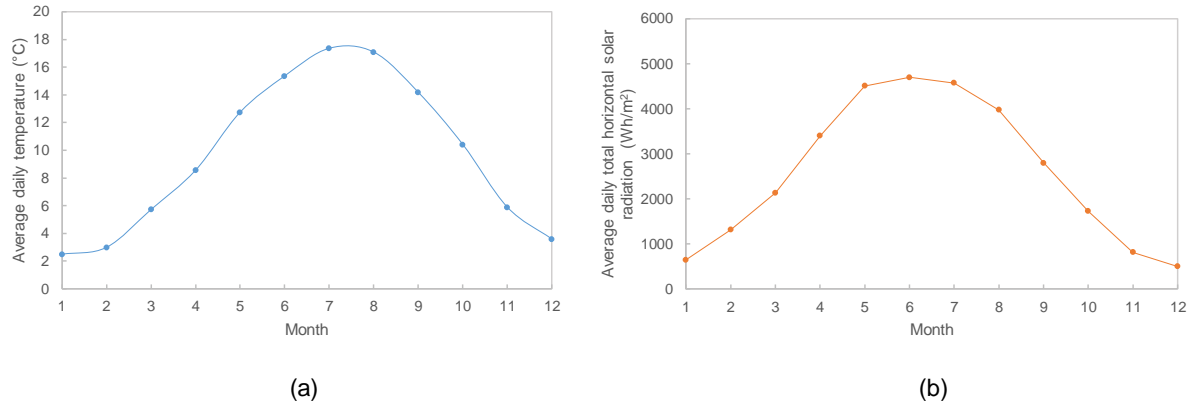


**Figure 16- Average daily temperature per month (a) and average daily horizontal solar insolation per month (b)**

### 5.3 Thermal characteristics of the building components

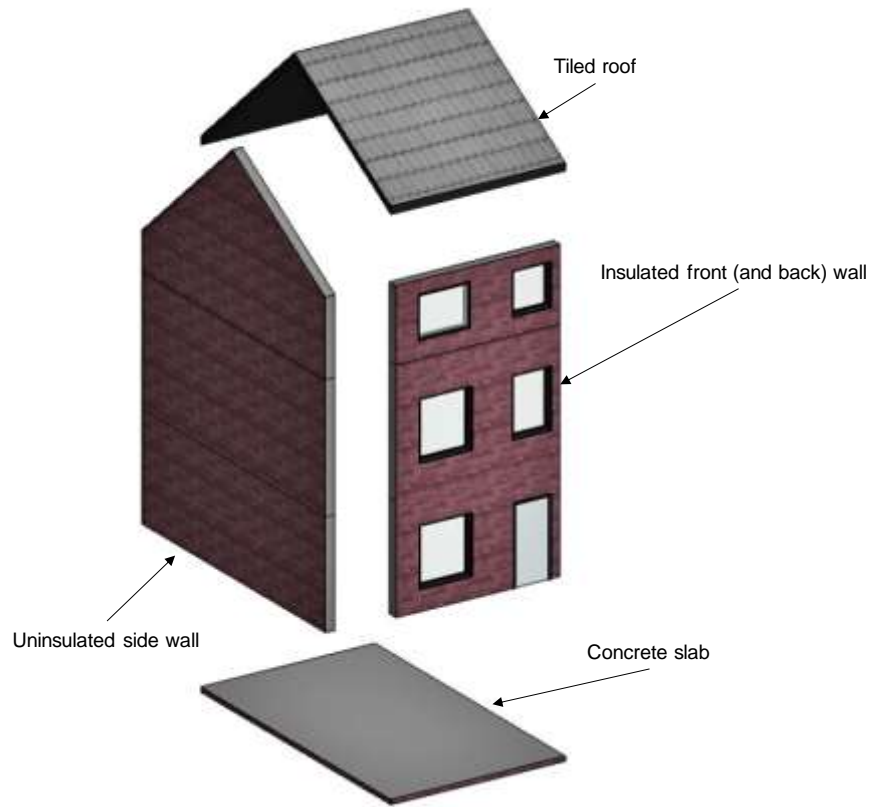


**Figure 17- Exploded view of the residential house**

The investigated Multilayered Building (MB) is composed of four main opaque components (Fig. 17):

- The front and back walls are 34 cm thick and insulated from the inside.
- The side walls are party walls in contact with adjacent buildings, they are 22 cm thick and are not insulated since they do not have a contact with the outdoor ambience.
- The slab is made of concrete and is not insulated.
- The roof has a wooden structure and is covered with roof tiles; it has a 10 cm insulation.

On the other hand, an Equivalent Building (EB) is similar to the Multilayered Building but with the difference of replacing the multilayered components (Front and back walls, Slab, and Roof) with the equivalent ones (Equivalent Wall, Equivalent Slab, Equivalent Roof).

Case 2 ( $\Theta \neq 0$ ) is considered since the heat flux  $\varphi_i$  (from the inside) and the constant temperature  $T_i$  are from the same side. The composition of the MB and the EB components is listed in Table 5, and the thermal properties of each layer are shown in Table 6. The equivalent thermal properties of the insulated walls, roof, and slab are determined using Eq. 4-16 and are presented in Table 7.

**Table 5- Multilayered and Equivalent Building components**

	MB		EB	
	Layers	Thickness (mm)	Layers	Thickness (mm)
Front and back walls	Gypsum board	15	Equivalent Wall	375
	Thermal insulation	20		
	Masonry brick	340		
Side walls	Masonry brick	200	-	-
Slab	Stone tiles	20	Equivalent Slab	250
	Mortar	30		
	Concrete	200		
Roof	Gypsum board	15	Equivalent Roof	135
	Thermal insulation	100		
	Roof tiles	20		

**Table 6- Thermal properties of the different building layers**

Layer	$\lambda$ (w.m <sup>-1</sup> .K <sup>-1</sup> )	$C_p$ (J.kg <sup>-1</sup> .K <sup>-1</sup> )	$\rho$ (kg.m <sup>-3</sup> )
Thermal insulation	0.04	800	40
Masonry brick	1	800	1000
Gypsum board	0.16	840	950
Stone tiles	3.06	1000	2500
Mortar	1.39	1000	2000
Concrete	2.10	800	2400
Roof tiles	1.15	900	1900

**Table 7- Equivalent thermal properties of the multilayered building components**

Equivalent wall	$\lambda$ (w.m <sup>-1</sup> .K <sup>-1</sup> )	$\rho C_p$ (J. m <sup>-3</sup> .K <sup>-1</sup> )	$e$ (m)
Wall	0.402	410241	0.375
Slab	2.03	1904756	0.25
Roof	0.0517	47078	0.135

#### 5.4 Comparison between the MB and the EB

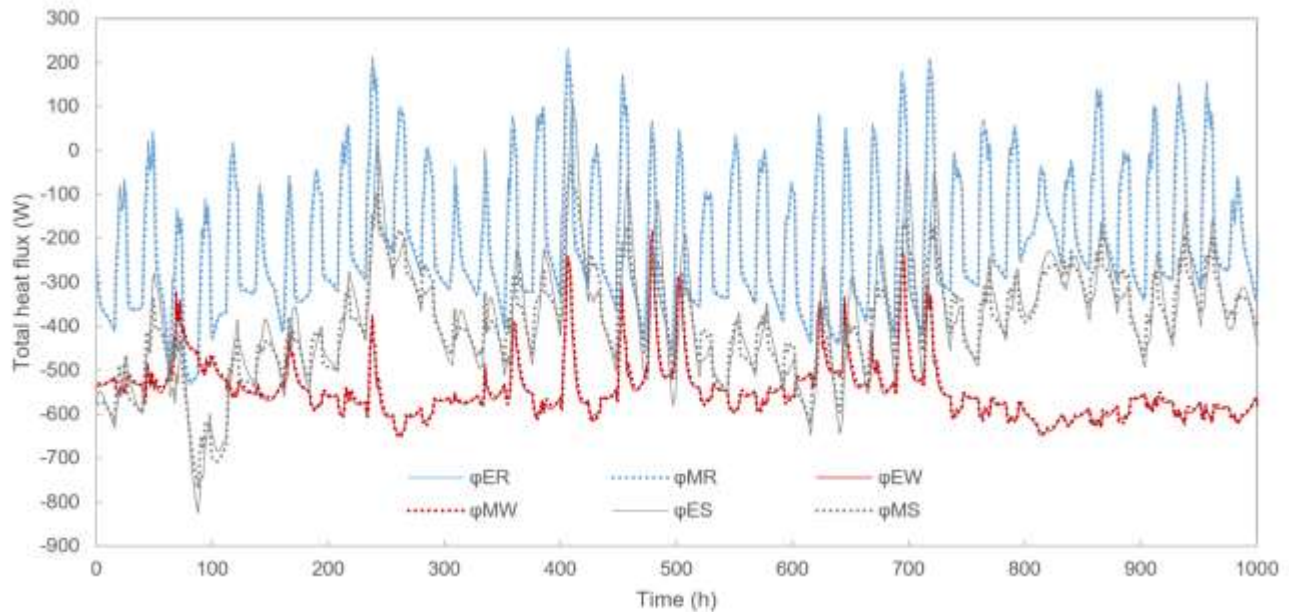


**Figure 18- Total heat flux through the walls, the slab, and the roof for the MB and the EB**

Fig. 18 shows the evolution of the total heat flux through the Multilayered Roof (MR), Multilayered Wall (MW), and Multilayered Slab (MS), compared to the Equivalent Roof (ER), Equivalent Wall (EW), and Equivalent Slab (ES) respectively for 1000 consecutive hours (42 days).

The evolution of the heat fluxes is very similar between the MB and the EB for all of the three components which confirms that the Equivalent Building model is reliable and can represent with a good accuracy the Multilayered Building. Moreover, one can conclude that using the proposed analytical methodology for determining the equivalent thermal properties of multilayered building components is accurate and that it is possible to assess the thermal performance of multilayered building components without knowing exactly the thermal properties of each layer. This simplifies the approaches used for characterizing existing multilayered building walls especially when dealing with old buildings where the thermal properties of their components is unknown.

## 6 Conclusion and recommendations

In this study two numerical methods were applied to an insulated tested masonry wall in random boundary conditions by generating a random temperature profile through a heating box. In the first method (sequential identification by layer), the thermal properties of each layer are computed by starting with the layer in direct contact with the measured heat flux. This method requires knowing the thicknesses of the different layers and the access to the interfaces between these layers to insert thermocouples; it is recommended when the thermal properties of each layer are needed. The second method (equivalent wall) considers an equivalent one-layer homogeneous wall that can generate a similar heat flux as the multilayered wall when subjected to similar boundary conditions. This method is simpler since it requires only the measurements at the interior and exterior wall sides, and is recommended when the overall thermal performance of the wall is needed.

The two methods give comparable results for the thermal characteristics of the wall with a difference of about 4% for  $\lambda$  and 10% for  $(\rho C_p)$ . The results were also validated by comparing them with the thermal properties of the masonry wall computed based on the experimental thermal characteristics of the blocks and mortar joints, as well as the experimental thermal characteristics of the polystyrene insulation.

An analytical analogy between the two methods is performed and a new method for determining the equivalent thermal properties of multilayered walls based on the thermal properties of each layer composing the multilayered wall is suggested.

A building case study model was finally studied to compare between the heat transfer in multilayered building elements (MB) and the equivalent building elements (EB). Similar heat fluxes profiles were obtained for the two building models through the different components (walls, roofs, and slabs) which proves that the equivalent building components can be used as accurate and reliable approach for simplifying the difficulty and complexity of thermal identification of multilayered existing building walls.

This study offered a new approach for understanding and characterizing the existing multilayered walls by using the concept of equivalent walls and the validation was performed numerically using a building case study and experimentally using an experimental masonry brick wall with polystyrene insulation in laboratory dynamic boundary conditions using a heating box. This method needs further validation using more experimental data in real weather conditions and thinner and lighter building components.

## References

- [1] Aimin Fang, Youming Chena, Lian Wu, “Transient simulation of coupled heat and moisture transfer through multilayer walls exposed to future climate in the hot and humid southern China Area”, *Sustainable Cities and Society* 52 (2020) 101812  
DOI: 10.1016/j.scs.2019.101812
- [2] Blaise Ravelo, Lala Rajaoarisoa, Olivier Maurice, “Thermal modelling of multilayer walls for building retrofitting applications”, *Journal of Building Engineering* 29 (2020) 101126  
DOI: 10.1016/j.jobe.2019.101126
- [3] B. Lacarriere, A. Trombe, F. Monchoux, “Experimental unsteady characterization of heat transfer in a multi-layer wall including air layers—Application to vertically perforated bricks”, *Energy and Buildings* 38 (2006) 232–237  
DOI: 10.1016/j.enbuild.2005.05.005
- [4] EN ISO 9869-1, Thermal Insulation – Building Elements – In-Situ Measurement of Thermal Resistance and Thermal Transmittance. Part 1: Heat Flow Meter Method, 2014.
- [5] R. Bruno, P. Bevilacqua, G. Cuconati, N. Arcuri, “An innovative compact facility for the measurement of the thermal properties of building materials: first experimental results”, *Applied Thermal Engineering* 143 (2018) 947-954  
DOI: 10.1016/j.applthermaleng.2018.06.023
- [6] L. Evangelisti, C. Guattari, F. Asdrubali, “Comparison between heat-flow meter and Air-Surface Temperature Ratio techniques for assembled panels thermal characterization”, *Energy & Buildings* 203 (2019) 109441  
DOI: 10.1016/j.enbuild.2019.109441
- [7] G. Desogus, S. Mura, R. Ricciu, “Comparing different approaches to in situ measurement of building components thermal resistance”, *Energy & Buildings* 43 (2011) 2613–2620  
DOI: 10.1016/j.enbuild.2011.05.025.
- [8] Eduardo Roque, Romeu Vicente, Ricardo M.S.F. Almeida, J. Mendes da Silva, Ana Vaz Ferreira, Thermal characterisation of traditional wall solution of built heritage using the simple hot box-heat flow meter method: in situ measurements and numerical simulation, *Applied Thermal Engineering* (2020)  
DOI: 10.1016/j.applthermaleng.2020.114935
- [9] David Bienvenido-Huertas, Carlos Rubio-Bellido, Juan Luis Perez-Ordenez, Miguel Jose Oliveira, “Automation and optimization of in-situ assessment of wall thermal transmittance using a Random Forest algorithm”, *Building and Environment* 168 (2020) 106479  
DOI: 10.1016/j.buildenv.2019.106479
- [10] Karthik A. Sabapathy, Sateesh Gedupudi, “In situ thermal characterization of rice straw envelope of an outdoor test room”, *Journal of Building Engineering* (2020)  
DOI: 10.1016/j.jobe.2020.101416
- [11] Xinrui Lu, Ali Memari, “Application of infrared thermography for in-situ determination of building envelope thermal properties”, *Journal of Building Engineering*, 26 (2019) 100885

DOI: 10.1016/j.job.2019.100885

[12] Muhammad Hafeez Abdul Nasir, Ahmad Sanusi Hassan, "Thermal performance of double brick wall construction on the building envelope of high-rise hotel in Malaysia", *Journal of Building Engineering* (2020)

DOI: 10.1016/j.job.2020.101389

[13] K. Chaffar, A. Chauchois, D. Defer, L. Zalewski, "Thermal characterization of homogeneous walls using inverse method", *Energy & Buildings* 78 (2014) 248-255

DOI: 10.1016/j.enbuild.2014.04.038

[14] A. J. Robinson, F. J. Lesage, A. Reilly, G. Mc Granaghan, G. Byrne, R. O'Hegarty, O. Kinnane, "A new transient method for determining thermal properties of wall sections", *Energy & Buildings* 142 (2017) 139-146

DOI: 10.1016/j.enbuild.2017.02.029

[15] Y. Yingying, T. V. Wu, A. Sempey, J. Dumoulin, J. C. Batsale, "Short time non-destructive evaluation of thermal performances of building walls by studying transient heat transfer", *Energy & Buildings* 184 (2019) 141–151

DOI: 10.1016/j.enbuild.2018.12.002

[16] G. Baldinelli, F. Bianchi, A. Lechowska, J. Schnotale, "Dynamic thermal properties of building components: Hot box experimental assessment under different solicitations", *Energy & Buildings* 168 (2018) 1–8

DOI: 10.1016/j.enbuild.2018.03.001

[17] R. Ricciu, A. Galatioto, L. Besalduch, S. Gana, A. Frattolillo, "Thermal properties of building walls: Indirect estimation using the inverse method with a harmonic approach", *Energy & Buildings* 187 (2019) 257–268

DOI: 10.1016/j.enbuild.2019.01.035

[18] EN ISO 13786, Thermal Performance of Building Components – Dynamic Thermal Characteristics – Calculation Methods, 2008.

[19] V. Gori, V. Marincioni, P. Biddulph, C. Elwell, "Inferring the thermal resistance and effective thermal mass distribution of a wall from in situ measurements to characterize heat transfer at both the interior and exterior surfaces", *Energy & Buildings* 135 (2017) 398–409

DOI: 10.1016/j.enbuild.2016.10.043

[20] Z. Petojević, R. Gospavić, G. Todorović, "Estimation of thermal impulse response of a multi-layer building wall through in-situ experimental measurements in a dynamic regime with applications", *Applied Energy* 228 (2018) 468–486

DOI: 10.1016/j.apenergy.2018.06.083

[21] Mihaela Teni, Hrvoje Krstic, Piotr Kosinski, "Review and comparison of current experimental approaches for in-situ measurements of building walls thermal transmittance", *Energy & Buildings*, 203 (2019) 109417

DOI: 10.1016/j.enbuild.2019.109417

[22] An-Heleen Deconinck, Staf Roels, "Comparison of characterisation methods determining the thermal resistance of building components from onsite measurements", *Energy and Buildings*, 130 (2016) 309–320

DOI: 10.1016/j.enbuild.2016.08.061

[23] Silvana Flores Larsen, Marcos Hongn, Nicolás Castro, Silvina González, “Comparison of four in-situ methods for the determination of walls thermal resistance in free-running buildings with alternating heat flux in different seasons”, *Construction and Building Materials*, 224 (2019) 455–473

DOI: 10.1016/j.conbuildmat.2019.07.033

[24] AgriMetSoft (2019). Online Calculators. Available on:

<https://agrimetsoft.com/calculators/Nash%20Sutcliffe%20model%20Efficiency%20coefficient>